
Online Transformers with Spiking Neurons for Fast Prosthetic Hand Control

N. Leroux

Peter Grünberg Institute,
Forschungszentrum Jülich,
Aachen, Germany
n.leroux@fz-juelich.de

J. Finkbeiner

Peter Grünberg Institute,
Forschungszentrum Jülich,
RWTH
Aachen, Germany
j.finkbeiner@fz-juelich.de

E. Neftci

Peter Grünberg Institute,
Forschungszentrum Jülich,
RWTH,
Aachen, Germany
e.neftci@fz-juelich.de

Abstract

Transformers are state-of-the-art networks for most sequence processing tasks. However, the self-attention mechanism often used in Transformers requires large time windows for each computation step and thus makes them less suitable for online signal processing compared to Recurrent Neural Networks (RNNs). In this paper, instead of the self-attention mechanism, we use a sliding window attention mechanism. We show that this mechanism is more efficient for continuous signals with finite-range dependencies between input and target, and that we can use it to process sequences element-by-element, this making it compatible with online processing. We test our model on a finger position regression dataset (NinaproDB8) with Surface Electromyographic (sEMG) signals measured on the forearm skin to estimate muscle activities. Our approach sets the new state-of-the-art in terms of accuracy on this dataset while requiring only very short time windows of 3.5 ms at each inference step. Moreover, we increase the sparsity of the network using Leaky-Integrate and Fire (LIF) units, a bio-inspired neuron model that activates sparsely in time solely when crossing a threshold. We thus reduce the number of synaptic operations up to a factor of $\times 5.3$ without loss of accuracy. Our results hold great promises for accurate and fast online processing of sEMG signals for smooth prosthetic hand control and is a step towards Transformers and Spiking Neural Networks (SNNs) co-integration for energy efficient temporal signal processing.

1 Introduction

Surface Electromyography (sEMG) is a technique that senses currents running through muscular fibers' membrane to measure muscular activity [1]. As sEMG signals are triggered by electrical stimuli from the central nervous system, this method is gaining a strong interest as a mean for Human-Machine Interfacing [1]. Since sEMG measurements only require electrodes positioned on the forearm skin, this technique is very promising for future non-invasive wearable prosthetic hand control system [1].

Transformers, which are the state-of-the-art networks for sequence processing [2, 3], can be very efficient to process sEMG signals [4]. However, the self-attention mechanism [2] used in conventional transformers requires to wait for large time windows, which induces a delay preventing fast online processing of continuous signals. Moreover, memory and computation of the self-attention mechanism scales quadratically with the sequence length.

In contrast, Recurrent Neural Networks (RNNs) integrate the concept of time into their operating model and are thus suited for continuous signals online processing. Spiking Neural Networks (SNNs) [5, 6] are a bio-inspired type of RNNs. They are very promising for low power applications because their neurons only transmit information when their membrane potential (an internal state of each neuron) reaches a threshold, and these events happen sparsely in time [6]. Many research focus on building new hardware that leverage the inherent temporal sparsity of SNNs [7, 8, 9, 10].

In this paper, we propose an online transformer that makes use of a linearized sliding window attention mechanism [11]. We adapt this attention mechanism for online processing of continuous signals by making it forward in time and serialized. Our online transformer thus performs inference for each token as they are generated. In order to leverage information from past inputs, we store information in the keys and the values of the attention mechanism, and we update this memory dynamically as the tokens are generated. The length of the sequences stored in the keys and the values is a hyper-parameter that we can tune to change the temporal depth of the information used in the attention mechanism, as well as the computational complexity and the memory usage.

We test our model on a finger position regression through sEMG signals using the Non-Invasive Adaptive Hand Prosthetics Database 8 (NinaProDB8) dataset. First, we show that our online transformer allows users to process sEMG signals with high accuracy using solely very short time windows of 3.5 ms, which permits a very fine granularity in time of prosthetic hand control. Secondly, we show that selecting the temporal depth of the attention improves the results of signal processing and makes our model outperform a self-attention-based transformer, as well as previous state-of-the-art models. Finally, we show how our custom online attention mechanism allows us to SNNs inside the transformer architecture to increase the network sparsity, which in turn results in a reduction of the required number of synaptic operations by a factor of $\times 5.3$ without loss of accuracy.

2 Related work

Deep Learning for Surface Electromyography processing Although sEMG signals and muscle activity are correlated, their relation is unknown and processing sEMG signals remains very challenging because of electrical noise (e.g., interference, ground noise, crosstalk between electrodes), inter-subject variability (e.g., different forearm circumferences, muscle characteristics), and intra-subject variability (e.g., variation of the electrodes position or the skin conductivity from one day to the next) [12].

Deep learning methods can leverage large datasets to extract the more relevant features despite noise or variability [13]. They can thus outperform conventional machine learning techniques like Support Vector Machine (SVM) [14]. Moreover, deep networks can process raw sEMG signals whereas conventional networks require prior pre-processing like Principal Component Analysis [15], Linear Discriminant Analysis (LDA) [15], Fourier transforms [16], and others.

Deep learning has already been applied to sEMG signals processing using Temporal Convolutions [17, 18, 19] and Recurrent Neural Networks (RNNs) [20, 21, 22, 23]. While the ability to compute on the edge with restricted memory capacity and low power consumption are essential to the deployment of autonomous wearable prosthetic hand control systems, most deep learning techniques are computationally intensive. Mukhopadhyay et al. [24] have shown that the inherent sparsity of SNNs can be leveraged to reduce drastically the computational intensity of sEMG signals processing. Burrello et al. [4] have shown that a transformer network can process sEMG signals with a limited memory usage and reduced number of Multiply-And-Accumulate (MAC) operations.

Transformers Unlike RNNs, Transformers do not suffer from the vanishing gradient problem for learning features in time [3], they do not have inductive biases made from assumptions about the data structure, and they can be trained very fast on GPUs since they can process an entire temporal sequence in parallel. The workhorse of Transformers is the self-attention mechanism, an operation that allows all the elements of a sequence to be compared with each other's. For Natural Language

Processing (NLP), the strength of self-attention is that it allows one token to be compared with present, past, and future tokens [2]. However, depending on the application, conventional self-attention is not always the best choice. It has been shown that using local attention and sliding windows attention can lead to better results for long sequences in NLP [11] and in Machine Vision [25].

Transformers with Spiking Neural Networks. SNNs, which mimic biological neural networks, are very promising for low power applications because their neurons only transmit information when their membrane potential (an internal state of each neuron) reaches a threshold, and these events happen sparsely in time [6]. Integrating SNNs in a transformer architecture is challenging and not intuitive. Just as RNNs, SNNs have a temporal dynamic. Thus, each element of a sequence must be fed to RNNs or SNNs sequentially. In contrast, since the self-attention mechanism compares all the different elements of a sequence in parallel, Transformers require to wait for the completion of a sequence before computing. For instance, the transformer used in [4] for sEMG classification used time windows of 150 ms. Naively stacking conventional self-attention layers and recurrent layers would then lead to undesirable delays due to the alteration between waiting time windows and processing sequences sequentially.

Yao et al. [26] have used a type of attention mechanism to select the importance of event frames, and then process the events with a SNN. Sabater et al. [27] have shown that a transformer can be used to process event-based vision sensor data more efficiently and accurately than convolutional neural networks. Zhou et al. [28] have used binarized self-attention to integrate sparsity in Transformers. Li et al. [29] have used a SNN as a pre-processing step for a transformer. It was also shown by Gehrig and Scaramuzza [30] that Long-Term Short-Term (LSTM) units can be integrated inside a transformer architecture, but in this work the attention mechanism was spatial and not temporal. Finally, Zhu et al. [31] have integrated spiking neurons inside a transformer architecture, but by using a custom attention mechanism that cannot be computed online.

In this paper, we introduce a transformer model that can perform attention in time online, and is compatible with spiking neurons at every layer of the architecture.

3 Methods

3.1 NinaproDB8: A Finger Position Regression Dataset

In this work, we used the Non-Invasive Adaptive Hand Prosthetics Database 8 (NinaProDB8) [12], a public sEMG database made as a benchmark for estimation of kinematic finger position. Many deep learning efforts applied to sEMG focus on simple functional movement classification [1, 4, 17, 18]. However, sequence-to-sequence regression of finger position can lead to a wider range of gestures and can be more easily coupled to sensory feedback from robotic hands for a closed-loop precise control [33].

The measurements of the database were made on 10 able-bodied subjects and two right trans-radial amputees. The sEMG signal, that is the input of our neural network (see Fig. 1 (a)), are recorded using 16 electrodes (Delsys Trigno IM Wireless EMG system) positioned around the right forearm of the participants. The finger positions were measured using a dataglove, the Cyberglove II, 18-Degrees of Freedom (DoF) model, that measures the finger-joint angles that correspond to the dots in Fig. 1 (b). The sEMG signals and the dataglove signals were up sampled to 2 kHz and post-synchronized. The details of the dataset can be found in [12].

In order to disregard the irrelevant degrees of freedom and focus directly on motions relevant for prosthetic hand control, it has been shown by Krasoulis et al. [12] that we can convert the 18-DoF recorded by the dataglove into 5-Degrees of Actuation (DoA) using a simple linear transformation. The matrix used for this linear transformation can be found in the supplementary materials of Krasoulis et al. [12]. We used the DoA as targets of our neural network.

Three datasets were recorded for each participant: the first two datasets (acquisition 1 and 2) comprised 10 repetitions of each movement and the third dataset (acquisition 3) comprised only 2 repetitions. We used both acquisition 1 and 2 as training set and acquisition 3 as testing set. In Fig. 1 (a) and (c) we show the example of the testing set for subject 1 (target).

To facilitate the training of our neural network, we normalize each set of repetition by subtracting the sEMG signals by their mean and dividing by their standard deviation.

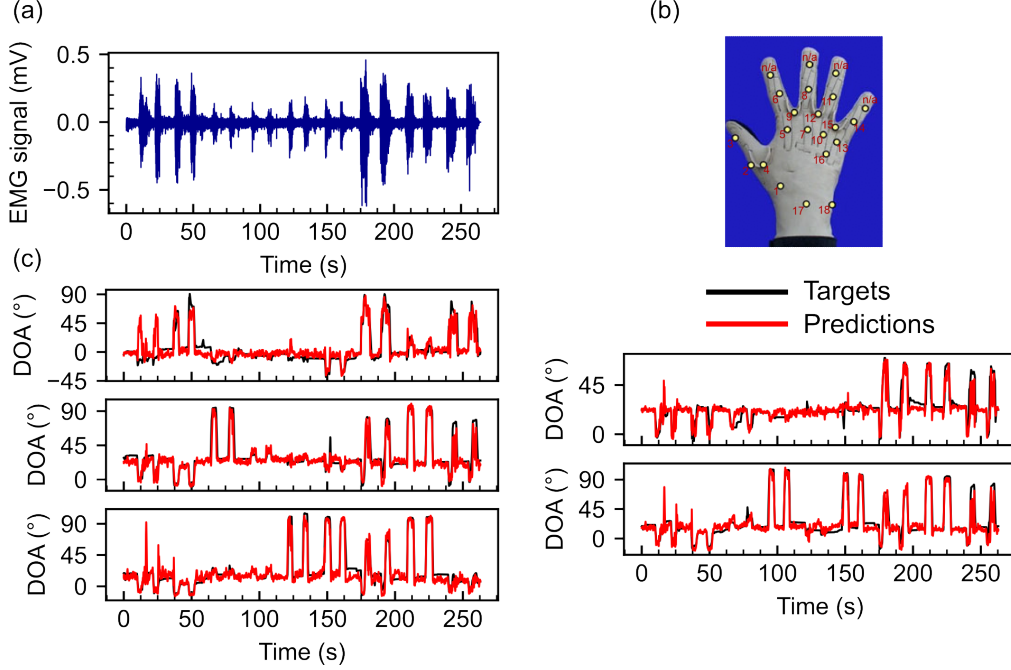


Figure 1: (a) Surface electromyography signal acquired using a 16 channel Delsys Trigno IM Wireless EMG system (see Krasoulis et al. [12]). The signal of only one out of the 16 channels is plotted. (b) The Cyberglove II is used for the acquisition of the ground truth finger-joint angles [32]. (c) Ground truth finger-joint angles and reconstruction with our Online Transformer model.

3.2 Online Inference with a Custom Attention Mechanism

In conventional transformers [2], the entire self-attention stage is calculated in parallel. The elements of the input sequence of a self-attention layer are called tokens, and the operation of self-attention is described as

$$\text{Attention}(Q, K, V) = \text{softmax}\left(\frac{Q \circ K^T}{\sqrt{d}}\right) \circ V \quad (1)$$

where \circ is the dot-product operator, $Q \in \mathbb{R}^{N \times d}$, $K \in \mathbb{R}^{N \times d}$, and $V \in \mathbb{R}^{N \times d}$ are respectively called the queries, the keys, and the values and are three different projections of the same sequence of tokens:

$$Q = W_Q x \quad (2a)$$

$$K = W_K x \quad (2b)$$

$$V = W_V x. \quad (2c)$$

The attention dimension d is the size of each token projection and N is the sequence length. $W_Q \in \mathbb{R}^{d \times D}$, $W_K \in \mathbb{R}^{d \times D}$, and $W_V \in \mathbb{R}^{d \times D}$ are learnable weights matrices with D the embedding dimension, and $x \in \mathbb{R}^{N \times D}$ the input of the attention mechanism.

In the case of continuous signals (such as bio-medical signals), it is possible to split the input signal into finite time windows, and to wait for the end of each time window before carrying-out the inference (as in Burrello et al. [4]). However, this method induces delays due to waiting for the end of the time windows. Our online transformer uses a custom attention mechanism that can be computed online for each element of the sequence without delays.

To avoid waiting for future tokens, the tokens of time step t_0 are not compared with future tokens of time steps $t > t_0$. The information from previous tokens is stored in the keys and the values $K \in \mathbb{R}^{M \times d}$ and $V \in \mathbb{R}^{M \times d}$. Unlike for self-attention, here the size of K and V does not depend on the full sequence length, but solely on M , which is the number past time steps we choose to store.

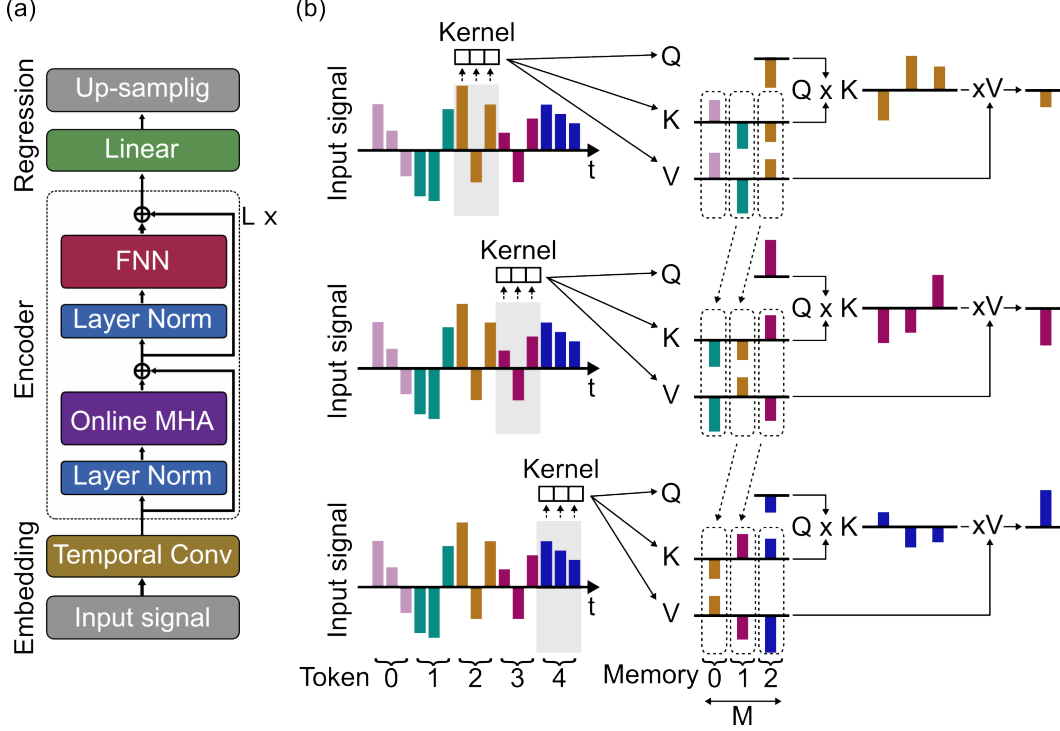


Figure 2: (a) Online Transformer neural network architecture. (b) Online Attention sketch: The different tokens are created by a temporal convolution (with a kernel size 3 and a stride 2 in this example). The tokens are linearly projected toward the queries, the keys and the values (\$Q\$, \$K\$, \$V\$). \$Q\$ matches only the present token whereas \$K\$ and \$V\$ store multiple previous tokens. The length \$M\$ of this memory is 3 in this example. At each time step, \$K\$ and \$V\$ forget the projection of the oldest token and store the projection of the new one. The mathematical operations of the online attention mechanism are described in section 3.2.

\$K\$ and \$V\$ are initially zeroed. Then, the elements \$K_i \in \mathbb{R}^d\$ and \$V_i \in \mathbb{R}^d\$ are iteratively replaced token-wise using the projections of Eqs. 2b and 2c. At each time step, a single query \$Q_t \in \mathbb{R}^d\$ is also computed with Eq. 2a, and the attention is computed as

$$\text{Attention}_t = \text{softmax} \left(\frac{Q_t \circ K}{\sqrt{d}} \right) \circ V \quad (3)$$

The softmax is computed on the memory length dimension \$M\$. Since one different element of \$K\$ and \$V\$ is updated at each time step, and since the length of \$K\$ and \$V\$ is \$M\$, all their elements are updated with a frequency \$\frac{1}{M}\$. The above-mentioned procedure is summarized as the Algorithm 1.

In contrast to the quadratic dependence with respect to sequence length for conventional self-attention (\$O(N^2)\$), the computational complexity of the sliding window attention mechanism is linear (\$O(MN)\$).

Eq. 3 shows that our attention mechanism can be computed time step wise instead of waiting for the end of large time windows to compute the attention in parallel. Now, we will show how this attention mechanism fits in our full neural network.

3.3 Neural Network Architecture

Our neural network consists of three blocks as depicted in Fig. 2 (a): an embedding block that converts the raw EMG signal into a sequence of tokens, an encoder block that uses attention to find correlation between sequence elements, and a regression block that converts the output into five degrees of actuation.

Algorithm 1 Inference with Online Attention

```

 $K = \mathbf{0}$   $\triangleright K \in \mathbb{R}^{M \times d}$ 
 $V = \mathbf{0}$   $\triangleright V \in \mathbb{R}^{M \times d}$ 
 $t = 0$ 
 $i = 0$ 
repeat
   $Q_t \leftarrow W_Q x_t$   $\triangleright Q_t \in \mathbb{R}^d$ 
   $K_i \leftarrow W_K x_t$   $\triangleright K_i \in \mathbb{R}^d$ 
   $V_i \leftarrow W_V x_t$   $\triangleright V_i \in \mathbb{R}^d$ 
   $\text{Attention}_t \leftarrow \text{softmax} \left( \frac{Q_t \circ K}{\sqrt{d}} \right) \circ V$ 
   $t \leftarrow t + 1$   $\triangleright$  New time step
   $i \leftarrow i + 1$ 
   $i \leftarrow i \pmod{M}$ 
until end of sequence
  
```

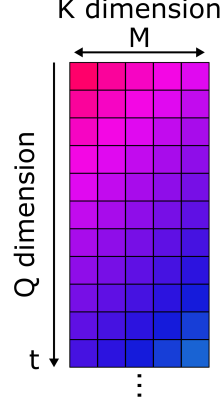


Figure 3: Sliding window attention. The same K values are represented by the same colors.

The embedding is made of a temporal convolution layer. Convolutional layers have overlaps between input time windows, which means that unlike linear layers, they have an intrinsic order, and thus do not require positional embeddings [2]. The convolutional layer has $C = 16$ input channels matching the 16 electrodes, and $D = 64$ output channels. The network is tested with kernels of various sizes to vary the length of the input time window that matches one token. We chose to make an overlap of two time steps between time windows, which makes the convolutional layer stride be $s = k - 2$, where k is the kernel size. With a padding $p = 1$, the number of tokens generated thus depends on the stride as

$$N = \lfloor \frac{N_{\text{samples}}}{s} \rfloor \quad (4)$$

where N_{samples} is the number of processed samples of the input signal.

The encoder is described as

$$\begin{aligned} f(x) &= x + \text{MHA}(\text{LN}(x)) \\ z(f(x)) &= f(x) + \text{FNN}(\text{LN}(f(x))) \end{aligned} \quad (5)$$

where LN is a layer norm layer. MHA is the multi-head attention layer with $h = 8$ heads computed in parallel using Eq. 3, with an attention dimension $d = 32$. After that attention is computed, the h heads are concatenated and projected into dimension $D = 64$. FNN is a Feedforward Neural Network with one hidden layer of 128 GeLU units [34] and a dropout layer with probability 0.2. The linear projections of FNN are applied token-wise so that that they can be computed online. The entire encoder block can be repeated and stacked L times, but here we chose to keep $L = 1$. The backbone of our neural network is inspired from Burrello et al. [4].

Finally, the regression block consists of a linear layer that projects each token from a dimension $D = 64$ to a dimension 5 (the number of degrees of actuation we perform the regression on), and an up sampling layer that duplicates the output of each token to generate as many samples as there are in the target signal (an example of target signal is shown in Fig. 1 (c)). The up sampling factor is equal to the stride that we use in the convolutional embedding layer (see Eq. 4).

3.4 Increasing the network sparsity with binarization and spiking neurons

In order to reduce the number of required operations, we increase the network sparsity by using binarization and Leaky Integrate and Fire (LIF) units [5, 6] units. We test two sparse models. In the first one, we binarize the output of the convolutional embedding, we binarize the projections Q , K , and V , and we replace the FNN by a SNN with a first layer of 128 LIF units, and a second of $D = 64$ LIF units. The second sparse model is similar to the first one, but instead of binarizing Q , K , and V , we replace each projection of Eqs. 2a, 2b, and 2c by a single spiking layer of $d = 32$ LIF units, which adds an additional dynamic to the model.

Binarization is done by applying a Heaviside function. The dynamics of the LIF units are defined by

$$U_t = \alpha (1 - S_{t-1}) U_{t-1} + (1 - \alpha) I_{t-1} \quad (6a)$$

$$I_t = \beta I_{t-1} + (1 - \beta) W x_t \quad (6b)$$

$$S_t = H(U_{t-1} - \Theta) \quad (6c)$$

where t is the index of the tokens, U is the membrane potential, I is the synaptic current, S is the spike response, H is the Heaviside function, $\alpha = 0.95$, $\beta = 0.9$, and $\Theta = 1$. The outputs of the Q , K , and V projections are the spike responses S_t (see Eq. 6c). The outputs of the first layer of the SNN replacing the FNN are the spike responses S_t , and the outputs of the second layer are the membrane potentials U_t (see Eq. 6a).

Because the Heaviside function is not differentiable, during training the gradient of the different Heaviside functions (used for binarization and LIF units) are replaced by the SuperSpike surrogate gradient [5, 35]. To preserve the sparsity between the embedding and the encoder block, we remove the layer norm layer that precedes the embedding when the embedding is binarized. In addition, we remove the dropout layers in the two sparse models. The softmax of the attention mechanism is only computed on non-zero elements.

3.5 Training

To speed up training, the attention block is computed in parallel. Projections $Q \in \mathbb{R}^{N \times d}$, $K \in \mathbb{R}^{N \times d}$, and $V \in \mathbb{R}^{N \times d}$ are computed for an entire time window with N tokens. The keys and values are then unfolded into sliding windows of size M and stride 1, similarly as for a convolution (see in Fig. 3 an example of sliding window attention). The product between queries and keys is thus computed as

$$\begin{bmatrix} Q_0 K_{1-M} & \cdots & Q_0 K_{-2} & Q_0 K_{-1} & Q_0 K_0 \\ Q_1 K_{2-M} & \cdots & Q_1 K_{-1} & Q_1 K_0 & Q_1 K_1 \\ Q_2 K_{3-M} & \cdots & Q_2 K_0 & Q_2 K_1 & Q_2 K_2 \\ \vdots & \ddots & \vdots & \vdots & \vdots \\ Q_N K_{N-M} & \cdots & Q_N K_{N-3} & Q_N K_{N-2} & Q_N K_{N-1} \end{bmatrix}. \quad (7)$$

Since the keys $K_{i < 0}$ are forbidden values, we mask them by replacing them with $-\infty$ as in Vaswani et al. [2], so that they are not computed in the softmax (see Eq. 3). The values $V_{i < 0}$ are simply zeroed.

To improve training, we developed a simple data augmentation protocol: first, the training set signals are sliced into time windows of $N_{\text{samples}} = 2000$ samples (which corresponds to 1 s since the sampling rate is 2 kHz). Then, each time window is duplicated 64 times. For data augmentation, the beginning of each of this duplicated time window is shifted with a random number sampled in a uniform distribution between 0 and 2000. Finally, the resulting time windows are shuffled to create the training dataset.

We trained each network for each subject for 10 epochs using the Adam optimizer [36], a learning rate of 10^{-3} , batch sizes of 64, and since the metric we want to minimize is the mean average error (MAE) over the 5 degrees of freedom (DoA), we used the L1 loss function.

For the sparse models, we added a sparsity loss function term [37] to the global loss to increase the sparsity of the embedding, the queries, keys and values such that the total loss is:

$$\mathcal{L}(y, \hat{y}) = \|y_{i,j} - \hat{y}_{i,j}\|_1 - \frac{1}{2} \lambda (\|x\|_2 + \|\text{Concat}(Q, K, V)\|_2) \quad (8)$$

with y the network outputs, \hat{y} the targets, x the embeddings and $\lambda = 1$.

In this study, we simply trained and tested datasets independently for each subject. To improve accuracy and repeatability in future studies, it is also possible to use transfer learning: the network can learn from multiple subjects before fine-tuning and testing on a new subject, as in [38].

4 Results

In Fig. 1 (c) we show an example of the regression results for a sparse online transformer with a embedding convolution kernel size $k = 7$ and a memory length $M = 150$. We first investigate how k

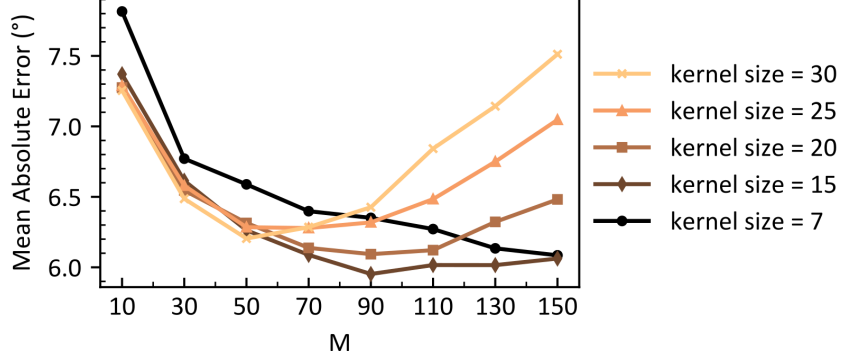


Figure 4: Mean absolute error averaged over the 12 subjects versus the number of stored tokens M for kernel embedding sizes of 7, 15, 20, 25, and 30 (from black to light yellow curves).

and M affect the final accuracy. For this study, we use the network without sparsity. Since $s = k - 2$, we simultaneously change s and k , and thus the number of tokens N generated for a given time window (see Eq. 4). The memory length M defines how many past tokens are used in the attention mechanism. The time length of the signal used to store information in K and V is thus:

$$\tau_{\text{memory}} = \frac{M \times s}{\text{SamplingRate}}. \quad (9)$$

In Fig. 4 we plot the mean absolute error (MAE) over the different degrees of actuation for values of M swept between 10 and 150 with intervals of 20, and for five different values $k = 7, 15, 20, 25$, and 30 (which correspond to $s = 5, 13, 18, 23$ and 28). While sweeping M , we see for $k = 15, 20, 25$, and 30 that the MAE reaches a minimum and then increases. It shows that there is then an optimum value of memory length for each kernel size, and we see that this optimum value decreases with the kernel size and thus with the stride. Using Eq. 9, this result indicates that there is an optimum length of information τ_{memory} used in the attention mechanism, and that past that point increasing the stored information does not increase the accuracy. Then, we compare our different models using each time a kernel size $k = 7$ and a memory length is $M = 150$. As we see in Fig 4, these parameters lead to the best accuracy using the shortest time window for each token. For this study we also measure the 10°-accuracy and the 15°-accuracy, which are respectively the proportion of time samples that lead to mean average errors inferior to ten and fifteen degrees [21]. These additional metrics are important to measure the accuracy of the prediction within a margin of error. The different results are shown in Table 4. The mean and standard deviation of each metric are computed over the 12 subjects of the NinaproDB8 dataset.

To see the impact on our online transformer with custom sliding window attention mechanism, we compare it to a conventional Transformer with self-attention. For the three metrics, our online transformers outperform the transformer with conventional self-attention (see Table 4). This results further reveals the importance of selecting relevant information, and that for sEMG signal processing, it is likely more important to use local information from the past than global information from both past and future.

Our two sparse models reach similar accuracy than our non-sparse online transformer (and thus also better accuracy than equivalent conventional transformer), and respectively lead to a reduction of the number of required Multiply-And-Accumulate operations (MAC ops) by factors of $3.8\times$ and $5.3\times$ compared to the non-sparse online transformer (the activation function operations are not included in these calculations). The method used to compute the number of required operations is described in the Appendix.

Moreover, we see that our three online transformer models outperform LSTMs [21] by at least 0.88° of MAE, outperform Temporal Convolutions [19] with at least 0.76° of MAE (previous SoTA on NinaproDB8 dataset). To compare the inference speed of the different methods, we define the minimum time of computing as the length of the time windows used for each inference step, which for our online transformer is $\tau_{\text{min}} = \frac{k}{\text{SamplingRate}}$, with k the embedding convolution kernel size. Since $k = 7$ and the sampling rate is 2 kHz, our network can compute with a minimum latency of

Table 1: Results of regression on the Ninapro DB8 database with different models

Model	MAE (°)↓	10°-accuracy↑	15°-accuracy↑	τ_{\min} ↓	MMAC ops.↓ /inference
SVM* [19]	7.28	0.79	0.88	60 ms	–
MLP* [19]	7.14	0.80	0.89	60 ms	–
TempConv [19]	6.89	0.81	0.90	128 ms	3.2
LSTM [21]	7.04	–	–	10 ms	–
Transformer [†]	6.62±1.52	0.87±0.07	0.92±0.05	2 s	3,769
Online Transformer [†]	6.10±1.50	0.86±0.07	0.94±0.05	3.5 ms	5.3
Online Transformer with binary embedding and QKV, spiking FNN [†]	6.08±1.27	0.87±0.06	0.94±0.04	3.5 ms	1.4
Online Transformer with binary embedding, spiking QKV and FNN [†]	6.16±1.39	0.87±0.07	0.94±0.04	3.5 ms	1.0

* With prior feature extraction.
[†] This work.

3.5 ms, which is shorter than any previous methods and in particular more than $30\times$ shorter than the Temporal Convolutional network [19] which was the previous SoTA for the Ninapro DB8 dataset.

5 Conclusion

In this work, we developed an online transformer model that leverages sliding window attention to process tokens one at the time. We have shown that the locality of the sliding window makes it more efficient than self-attention. The proposed method makes sEMG signal processing with very short time windows (3.5 ms) possible, and sets the new state-of-the-art on the prosthetic hand control NinaproDB8 dataset. Using sliding window attention, our model also solves the problem of the integration of SNNs temporal dynamics in Transformers. We used a combination of binarization and SNNs to increase the network sparsity, thus reducing the number of required operation up to a factor $5.3\times$. In conclusion, this work is a step toward precise, smooth, and low-power Human-Machine Interfacing, and holds great promises for future neuromorphic transformer models.

References

- [1] Mingde Zheng, Michael S. Crouch, and Michael S. Eggleston. Surface electromyography as a natural human-machine interface: A review. 22(10):9198–9214. ISSN 1558-1748. doi: 10.1109/JSEN.2022.3165988. Conference Name: IEEE Sensors Journal.
- [2] Ashish Vaswani, Noam Shazeer, Niki Parmar, Jakob Uszkoreit, Llion Jones, Aidan N Gomez, Łukasz Kaiser, and Illia Polosukhin. Attention is all you need. In *Advances in Neural Information Processing Systems*, volume 30. Curran Associates, Inc. URL <https://papers.nips.cc/paper/2017/hash/3f5ee243547dee91fbd053c1c4a845aa-Abstract.html>.
- [3] Tianyang Lin, Yuxin Wang, Xiangyang Liu, and Xipeng Qiu. A survey of transformers. 3:111–132. ISSN 2666-6510. doi: 10.1016/j.aiopen.2022.10.001. URL <https://www.sciencedirect.com/science/article/pii/S2666651022000146>.
- [4] Alessio Burrello, Francesco Bianco Morghet, Moritz Scherer, Simone Benatti, Luca Benini, Enrico Macii, Massimo Poncino, and Daniele Jahier Pagliari. Bioformers: Embedding transformers for ultra-low power sEMG-based gesture recognition. In *2022 Design, Automation & Test in Europe Conference & Exhibition (DATE)*, pages 1443–1448. doi: 10.23919/DATE54114.2022.9774639. ISSN: 1558-1101.

Python codes available at <https://github.com/NathanLeroux-git/OnlineTransformerWithSpikingNeurons>

- [5] Friedemann Zenke and Surya Ganguli. SuperSpike: Supervised learning in multilayer spiking neural networks. 30(6):1514–1541. ISSN 0899-7667. doi: 10.1162/neco_a_01086. URL https://doi.org/10.1162/neco_a_01086.
- [6] Amirhossein Tavanaei, Masoud Ghodrati, Saeed Reza Kheradpisheh, Timothée Masquelier, and Anthony Maida. Deep learning in spiking neural networks. 111:47–63. ISSN 0893-6080. doi: 10.1016/j.neunet.2018.12.002. URL <https://www.sciencedirect.com/science/article/pii/S0893608018303332>.
- [7] Paul A. Merolla, John V. Arthur, Rodrigo Alvarez-Icaza, Andrew S. Cassidy, Jun Sawada, Filipp Akopyan, Bryan L. Jackson, Nabil Imam, Chen Guo, Yutaka Nakamura, Bernard Brezzo, Ivan Vo, Steven K. Esser, Rathinakumar Appuswamy, Brian Taba, Arnon Amir, Myron D. Flickner, William P. Risk, Rajit Manohar, and Dharmendra S. Modha. A million spiking-neuron integrated circuit with a scalable communication network and interface. 345(6197): 668–673. ISSN 0036-8075, 1095-9203. doi: 10.1126/science.1254642. URL <https://science.sciencemag.org/content/345/6197/668>. Number: 6197 Publisher: American Association for the Advancement of Science Section: Report.
- [8] Chen Liu, Guillaume Bellec, Bernhard Vogginger, David Kappel, Johannes Partzsch, Felix Neumärker, Sebastian Höppner, Wolfgang Maass, Steve B. Furber, Robert Legenstein, and Christian G. Mayr. Memory-efficient deep learning on a SpiNNaker 2 prototype. 12. ISSN 1662-453X. URL <https://www.frontiersin.org/articles/10.3389/fnins.2018.00840>.
- [9] Garrick Orchard, E. Paxon Frady, Daniel Ben Dayan Rubin, Sophia Sanborn, Sumit Bam Shrestha, Friedrich T. Sommer, and Mike Davies. Efficient neuromorphic signal processing with loihi 2. In *2021 IEEE Workshop on Signal Processing Systems (SiPS)*, pages 254–259. doi: 10.1109/SiPS52927.2021.00053. ISSN: 2374-7390.
- [10] Christian Pehle, Sebastian Billaudelle, Benjamin Cramer, Jakob Kaiser, Korbinian Schreiber, Yannik Stradmann, Johannes Weis, Aron Leibfried, Eric Müller, and Johannes Schemmel. The BrainScaleS-2 accelerated neuromorphic system with hybrid plasticity. 16:795876. ISSN 1662-4548. doi: 10.3389/fnins.2022.795876. URL <https://www.ncbi.nlm.nih.gov/pmc/articles/PMC8907969/>.
- [11] Iz Beltagy, Matthew E. Peters, and Arman Cohan. Longformer: The long-document transformer. URL <http://arxiv.org/abs/2004.05150>.
- [12] Agamemnon Krasoulis, Sethu Vijayakumar, and Kianoush Nazarpour. Effect of user practice on prosthetic finger control with an intuitive myoelectric decoder. 13. ISSN 1662-453X. URL <https://www.frontiersin.org/articles/10.3389/fnins.2019.00891>.
- [13] Andrés Jaramillo-Yáñez, Marco E. Benalcázar, and Elisa Mena-Maldonado. Real-time hand gesture recognition using surface electromyography and machine learning: A systematic literature review. 20(9):2467. ISSN 1424-8220. doi: 10.3390/s20092467. URL <https://www.mdpi.com/1424-8220/20/9/2467>. Number: 9 Publisher: Multidisciplinary Digital Publishing Institute.
- [14] Bojan Milosevic, Elisabetta Farella, and Simone Benatti. Exploring arm posture and temporal variability in myoelectric hand gesture recognition. In *2018 7th IEEE International Conference on Biomedical Robotics and Biomechatronics (Biorob)*, pages 1032–1037. doi: 10.1109/BIOROB.2018.8487838. ISSN: 2155-1782.
- [15] Pornchai Phukpattaranont, Sirinee Thongpanja, Khairul Anam, Adel Al-Jumaily, and Chusak Limsakul. Evaluation of feature extraction techniques and classifiers for finger movement recognition using surface electromyography signal. 56(12):2259–2271. ISSN 1741-0444. doi: 10.1007/s11517-018-1857-5. URL <https://doi.org/10.1007/s11517-018-1857-5>.
- [16] Zahra Taghizadeh, Saeid Rashidi, and Ahmad Shalbaf. Finger movements classification based on fractional fourier transform coefficients extracted from surface EMG signals. 68:102573. ISSN 1746-8094. doi: 10.1016/j.bspc.2021.102573. URL <https://www.sciencedirect.com/science/article/pii/S1746809421001701>.

- [17] Panagiotis Tsinganos, Bruno Cornelis, Jan Cornelis, Bart Jansen, and Athanassios Skodras. Improved gesture recognition based on sEMG signals and TCN. In *ICASSP 2019 - 2019 IEEE International Conference on Acoustics, Speech and Signal Processing (ICASSP)*, pages 1169–1173. doi: 10.1109/ICASSP.2019.8683239. ISSN: 2379-190X.
- [18] Marcello Zanghieri, Simone Benatti, Alessio Burrello, Victor Kartsch, Francesco Conti, and Luca Benini. Robust real-time embedded EMG recognition framework using temporal convolutional networks on a multicore IoT processor. 14(2):244–256, . ISSN 1940-9990. doi: 10.1109/TBCAS.2019.2959160. Conference Name: IEEE Transactions on Biomedical Circuits and Systems.
- [19] Marcello Zanghieri, Simone Benatti, Alessio Burrello, Victor Javier Kartsch Morinigo, Roberto Meattini, Gianluca Palli, Claudio Melchiorri, and Luca Benini. sEMG-based regression of hand kinematics with temporal convolutional networks on a low-power edge microcontroller. In *2021 IEEE International Conference on Omni-Layer Intelligent Systems (COINS)*, pages 1–6, . doi: 10.1109/COINS51742.2021.9524188.
- [20] Khairul Anam, Cries Avian, Dwiretno Istiyadi Swasono, Aris Zainul Muttaqin, and Harun Ismail. Estimation of finger joint movement based on electromyography signal using long short-term memory. In *2020 International Conference on Computer Engineering, Network, and Intelligent Multimedia (CENIM)*, pages 86–90. doi: 10.1109/CENIM51130.2020.9298023.
- [21] Philipp Koch, Mark Dreier, Anna Larsen, Tim J. Parbs, Marco Maass, Huy Phan, and Alfred Mertins. Regression of hand movements from sEMG data with recurrent neural networks. In *2020 42nd Annual International Conference of the IEEE Engineering in Medicine & Biology Society (EMBC)*, pages 3783–3787. doi: 10.1109/EMBC44109.2020.9176278. ISSN: 2694-0604.
- [22] Zamroni Ilyas, Khairul Anam, Widjonarko, Cries Avian, Aris Zainul Muttaqin, and Mochammad Edoward Ramadhan. Evaluation of gated-recurrent unit for estimating finger-joint angle using surface electromyography signal. In *2022 9th International Conference on Electrical Engineering, Computer Science and Informatics (EECSI)*, pages 25–28. doi: 10.23919/EECSI56542.2022.9946461.
- [23] Jun Li, Lixin Wei, Yintang Wen, Xiaoguang Liu, and Hongrui Wang. An approach to continuous hand movement recognition using SEMG based on features fusion. . ISSN 0178-2789, 1432-2315. doi: 10.1007/s00371-022-02465-7. URL <https://link.springer.com/10.1007/s00371-022-02465-7>.
- [24] Anand Kumar Mukhopadhyay, Indrajit Chakrabarti, and Mrigank Sharad. Classification of hand movements by surface myoelectric signal using artificial-spiking neural network model. In *2018 IEEE SENSORS*, pages 1–4. doi: 10.1109/ICSENS.2018.8589757. ISSN: 2168-9229.
- [25] Ali Hassani and Humphrey Shi. Dilated neighborhood attention transformer. URL <http://arxiv.org/abs/2209.15001>.
- [26] Man Yao, Huanhuan Gao, Guangshe Zhao, Dingheng Wang, Yihan Lin, Zhaoxu Yang, and Guoqi Li. Temporal-wise attention spiking neural networks for event streams classification. pages 10221–10230. URL https://openaccess.thecvf.com/content/ICCV2021/html/Yao_Temporal-Wise_Attention_Spiking_Neural_Networks_for_Event_Streams_Classification_ICCV_2021_paper.html.
- [27] Alberto Sabater, Luis Montesano, and Ana C. Murillo. Event transformer. a sparse-aware solution for efficient event data processing. In *2022 IEEE/CVF Conference on Computer Vision and Pattern Recognition Workshops (CVPRW)*, pages 2676–2685. IEEE. ISBN 978-1-66548-739-9. doi: 10.1109/CVPRW56347.2022.00301. URL <https://ieeexplore.ieee.org/document/9857382/>.
- [28] Zhaokun Zhou, Yuesheng Zhu, Chao He, Yaowei Wang, Shuicheng Yan, Yonghong Tian, and Li Yuan. Spikformer: When spiking neural network meets transformer. URL <http://arxiv.org/abs/2209.15425>.

- [29] Yudong Li, Yunlin Lei, and Xu Yang. Spikeformer: A novel architecture for training high-performance low-latency spiking neural network, . URL <http://arxiv.org/abs/2211.10686>.
- [30] Mathias Gehrig and Davide Scaramuzza. Recurrent vision transformers for object detection with event cameras. URL <http://arxiv.org/abs/2212.05598>.
- [31] Rui-Jie Zhu, Qihang Zhao, and Jason K. Eshraghian. SpikeGPT: Generative pre-trained language model with spiking neural networks. URL <http://arxiv.org/abs/2302.13939>.
- [32] Stefano Pizzolato, Luca Tagliapietra, Matteo Cognolato, Monica Reggiani, Henning Müller, and Manfredo Atzori. Comparison of six electromyography acquisition setups on hand movement classification tasks. 12(10):e0186132. ISSN 1932-6203. doi: 10.1371/journal.pone.0186132. URL <https://dx.plos.org/10.1371/journal.pone.0186132>.
- [33] Marko Markovic, Meike A. Schweisfurth, Leonard F. Engels, Dario Farina, and Strahinja Dosen. Myocontrol is closed-loop control: incidental feedback is sufficient for scaling the prosthesis force in routine grasping. 15(1):81. ISSN 1743-0003. doi: 10.1186/s12984-018-0422-7. URL <https://doi.org/10.1186/s12984-018-0422-7>.
- [34] Dan Hendrycks and Kevin Gimpel. Gaussian error linear units (GELUs). URL <http://arxiv.org/abs/1606.08415>.
- [35] Emre O. Neftci, Hesham Mostafa, and Friedemann Zenke. Surrogate gradient learning in spiking neural networks: Bringing the power of gradient-based optimization to spiking neural networks. 36(6):51–63. ISSN 1558-0792. doi: 10.1109/MSP.2019.2931595. Number: 6 Conference Name: IEEE Signal Processing Magazine.
- [36] Diederik P. Kingma and Jimmy Ba. Adam: A method for stochastic optimization. URL <http://arxiv.org/abs/1412.6980>.
- [37] Yulong Yan, Haoming Chu, Yi Jin, Yuxiang Huan, Zhuo Zou, and Lirong Zheng. Backpropagation with sparsity regularization for spiking neural network learning. 16. ISSN 1662-453X. URL <https://www.frontiersin.org/articles/10.3389/fnins.2022.760298>.
- [38] Stephan Johann Lehmler, Muhammad Saif-ur Rehman, Tobias Glasmachers, and Ioannis Iossifidis. Deep transfer learning compared to subject-specific models for sEMG decoders. ISSN 1741-2560, 1741-2552. doi: 10.1088/1741-2552/ac9860. URL <https://iopscience.iop.org/article/10.1088/1741-2552/ac9860>.

A Appendix

To compute the number of synaptic MAC operations of our different models, we used the following set of equations, that represent the different operations (activation function excluded) of our models:

$$\# \text{EmbeddingMACs} = k \times C \times D \times 32 \quad (10a)$$

$$\# \text{QKVProjectionMACs} = (1 - \text{EmbeddingSparsity}) \times 3 \times D \times d \times h \times 32 \quad (10b)$$

$$\# \text{QKProductMACs} = \|QK\|_1 \times M \times h \times 32 \quad (10c)$$

$$\# \text{VProductMACs} = (1 - \text{VSparsity}) \times d \times M \times h \times 32 \quad (10d)$$

$$\# \text{ConcatMACs} = (1 - \text{AttentionSparsity}) \times d \times h \times D \times 32 \quad (10e)$$

$$\begin{aligned} \# \text{TotalAttentionMACs} = & \# \text{QKVProjectionMac} + \# \text{QKProductMacs} \\ & + \# \text{VProductMacs} + \# \text{ConcatMACs} \end{aligned} \quad (10f)$$

$$\# \text{FFL1MACs} = D \times H \times 32 \quad (10g)$$

$$\# \text{FFL2MACs} = (1 - \text{FFL1Sparsity}) \times H \times D \times 32 \quad (10h)$$

$$\# \text{RegressionMACs} = D \times 5 \times 32 \quad (10i)$$

$$\begin{aligned} \# \text{TotalMACs} = & \# \text{EmbeddingMacs} + \# \text{TotalAttentionMACs} \\ & + \# \text{FFL1MACs} + \# \text{FFL2MACs} + \# \text{RegressionMACs} \end{aligned} \quad (10j)$$